

# Imaging microglial activation and amyloid burden in amnesic mild cognitive impairment

Dunja Knezevic<sup>1,2</sup>, Nicolaas Paul LG Verhoeff<sup>1,3</sup>, Sina Hafizi<sup>1</sup>, Antonio P Strafella<sup>1,2,4</sup>, Ariel Graff-Guerrero<sup>1,2</sup>, Tarek Rajji<sup>1,2</sup>, Bruce G Pollock<sup>1,2</sup>, Sylvain Houle<sup>1,2</sup>, Pablo M Rusjan<sup>1,2</sup> and Romina Mizrahi<sup>1,2</sup>

## Abstract

Amnesic mild cognitive impairment (aMCI) is defined as a transitional state between normal aging and Alzheimer's disease (AD). Given the replicated finding of increased microglial activation in AD, we sought to investigate whether microglial activation is also elevated in aMCI and whether it is related to amyloid beta (A $\beta$ ) burden in-vivo. Eleven aMCI participants and 14 healthy volunteers completed positron emission tomography (PET) scans with [<sup>18</sup>F]-FEPPA and [<sup>11</sup>C]-PIB. Given the known sensitivity in affinity of second-generation TSPO radioligands, participants were genotyped for the TSPO polymorphism and only high-affinity binders were included. Dynamic [<sup>18</sup>F]-FEPPA PET images were analyzed using the 2-tissue compartment model with arterial plasma input function. Additionally, a supplementary method, the standardized uptake value ratio (SUVR), was explored. [<sup>11</sup>C]-PIB PET images were analyzed using the Logan graphical method. aMCI participants had significantly higher [<sup>11</sup>C]-PIB binding in the cortical regions. No significant differences in [<sup>18</sup>F]-FEPPA binding were observed between aMCI participants and healthy volunteers. In the aMCI group, [<sup>18</sup>F]-FEPPA and [<sup>11</sup>C]-PIB bindings were correlated in the hippocampus. There were no correlations between our PET measures and cognition. Our findings demonstrate that while A $\beta$  burden is evident in the aMCI stage, microglial activation may not be present.

## Keywords

Alzheimer's disease, amyloid, mild cognitive impairment, neuroinflammation, positron emission tomography

Received 5 April 2017; Revised 14 September 2017; Accepted 26 September 2017

## Introduction

Neuroinflammation and abnormal immunologic processes are important pathological features of Alzheimer's disease (AD);<sup>1</sup> however, the progression during disease course is not well understood. There has been increasing interest in studying mild cognitive impairment (MCI), which is defined as a transitional stage between normal aging and dementia.<sup>2</sup> Between the amnesic (aMCI) and non-amnesic subtypes (non-aMCI) of MCI, the former is more common and is thought to constitute the *prodromal* stage of AD, as individuals are at a higher risk of progression to AD.<sup>2,3</sup>

Microglia are resident phagocytes of the central nervous system (CNS) that provide the first line of defense against neuronal injuries/insults. Upon activation of

microglial cells, there is an increased expression of Translocator Protein 18 kDa (TSPO) on the outer layer of their mitochondria. This feature of TSPO makes it a valid target for in-vivo imaging of neuroinflammation with positron emission tomography (PET). The previous five PET studies investigating

<sup>1</sup>University of Toronto, Toronto, Ontario, Canada

<sup>2</sup>Centre for Addiction and Mental Health, Toronto, Ontario, Canada

<sup>3</sup>Baycrest Health Sciences, Toronto, Ontario, Canada

<sup>4</sup>Toronto Western Hospital, University Health Network, University of Toronto, Toronto, Ontario, Canada

## Corresponding author:

Romina Mizrahi, Centre for Addiction and Mental Health University of Toronto, Toronto, ON M5T 1R8, Canada.

Email: romina.mizrahi@camhpet.ca

neuroinflammation in prodromal individuals for AD have shown conflicting results. Out of the studies that have used the prototypical radioligand, [ $^{11}\text{C}$ ]-PK11195, two have demonstrated no differences in [ $^{11}\text{C}$ ]-PK11195 binding between healthy volunteers and MCI,<sup>4,5</sup> while one study with 14 aMCI patients found increased [ $^{11}\text{C}$ ]-PK11195 uptake in 38% of patients.<sup>6</sup> Given the known limitations of [ $^{11}\text{C}$ ]-PK11195 such as high nonspecific binding, low signal-to-noise ratio, and high plasma protein binding, there have been considerable efforts to develop improved radioligands. Second generation radioligands generally have higher affinity and brain uptake, and an improved signal-to-noise ratio compared with [ $^{11}\text{C}$ ]-PK11195; however, their binding affinity is influenced by a single nucleotide polymorphism (rs6971) in the TSPO gene.<sup>7</sup> Individuals can be classified as high-, mixed- and low affinity binders (HABs, MABs, and LABs, respectively). So far, two studies have investigated neuroinflammation with second-generation radioligands in MCI populations. The first study, using [ $^{11}\text{C}$ ]-DAA1106 in a population of seven MCI patients reported significant increases in binding relative to healthy volunteers.<sup>8</sup> An important caveat to consider is that the researchers did not have a purely amnesic sample (5 aMCI and 2 naMCI) and did not control for the rs6971 polymorphism. A latter study with [ $^{11}\text{C}$ ]-PBR28 reported no significant differences between aMCI and healthy volunteers.<sup>9</sup> This was the first to control for the effect of the TSPO genotype, in their 10 aMCI cohort, 4 were HAB and 6 were MABs. A recent study with [ $^{18}\text{F}$ ]-DPA714 in 64 AD patients demonstrated increased binding in the medium and posterior cingulate, precuneus, parietal and temporal cortex.<sup>10</sup> The researchers classified their AD patients into two groups according to their clinical dementia rating (CDR) score: 38 patients with a CDR score of 0.5 were classified as the prodromal AD group, while 26 patients with a CDR score of  $\geq 1$  constituted the AD dementia group. The increases in [ $^{18}\text{F}$ ]-DPA714 binding were observed in the prodromal AD group as well, without significant difference from the AD dementia group.

The accumulation of amyloid beta ( $\text{A}\beta$ ) plaques, one of the hallmarks of AD pathology, is believed to be a key factor that drives the neuroinflammatory process in AD.<sup>11</sup> Post-mortem immunohistochemical examinations of brain slices have demonstrated the presence of activated microglia clustered around  $\text{A}\beta$  plaques in AD.<sup>12-14</sup> This spatial relationship has been examined in-vivo with the use of radioligands that target amyloid, such as [ $^{11}\text{C}$ ]-PIB. Two studies with [ $^{11}\text{C}$ ]-PIB and [ $^{11}\text{C}$ ]-PK11195 did not find any regional correlations in AD and MCI populations,<sup>6,15</sup> whereas more recent studies with second-generation radioligands, [ $^{11}\text{C}$ ]-PBR28 and [ $^{18}\text{F}$ ]-DPA-714, demonstrated correlations

in regions of interest (ROI) when both prodromal AD and AD patients were grouped.<sup>9,10</sup>

The correlation of neuroinflammation with symptom severity and cognition is still unclear. Two MCI PET studies with [ $^{11}\text{C}$ ]-PK11195 reported no correlations with neuropsychological assessments.<sup>5,6</sup> In contrast, a study with [ $^{11}\text{C}$ ]-PBR28 in 19 AD and 10 aMCI patients reported a significant correlation between binding and impaired performance on measures of global cognition, memory, executive function and visuospatial abilities, however, only after partial volume correction and when the two patient populations were combined.<sup>9</sup> A more recent study with [ $^{18}\text{F}$ ]-DPA714 reported positive correlations between MMSE scores and global cortical binding in their combined sample of prodromal and AD participants.<sup>10</sup>

Given that previous studies have led to conflicting results, we sought to quantify microglial activation and amyloid burden with several methodological improvements. Firstly, we included a purely amnesic sample of MCI patients. Secondly, the use of a second-generation radioligand, [ $^{18}\text{F}$ ]-FEPPA, which has a high-affinity for TSPO, a good metabolic profile, high brain penetration and good pharmacokinetics.<sup>16</sup> A previous study with [ $^{18}\text{F}$ ]-FEPPA in AD, demonstrated an average of 48% higher binding in the cortical regions and 56% higher binding in the hippocampus of patients compared to healthy volunteer.<sup>1</sup> Thirdly, we used a high-resolution research tomograph scanner (HRRT). Lastly, we were the first to screen for the rs6971 polymorphism to include only HABs of both groups in the study, making our study the largest HAB population of participants.

## Methods

### Participants

Participants with aMCI were recruited from the memory clinics at Baycrest Health Sciences and the Centre for Addiction and Mental Health (CAMH), Toronto, Ontario. Healthy volunteers were recruited from the Baycrest Research Participant Database and from local advertisements. aMCI patients were diagnosed according to the Peterson et al.<sup>17</sup> criteria. The diagnosis of aMCI was made based on a consensus committee comprising neurologists, geriatric psychiatrists, neuropsychologists and other study personnel working at the memory clinics (CAMH and Baycrest).

Of over 300 individuals who were contacted for participation in the study, 83 individuals were interested and were screened over the phone. A total of 48 individuals met criteria and were invited for the screening visit whereby informed consent was obtained. Additionally, blood samples were collected for

genotyping of the TSPO polymorphism (rs6971). After genotyping, HABs of both groups were invited to proceed with the study. Eleven aMCI patients and 14 healthy volunteers completed the study procedures: a [ $^{18}\text{F}$ ]-FEPPA scan, a [ $^{11}\text{C}$ ]-PIB scan and an MRI scan. The exclusion criteria for aMCI and healthy volunteers included: concurrent Axis I disorders based on DSM-IV criteria, history of closed head injuries with loss of consciousness, strokes, or other neurological disorders with CNS involvement. All participants provided written informed consent. The protocol of this study was approved by the Research Ethics Boards of CAMH and Baycrest Health Sciences, and abided by the ethical guidelines set out by ICH GCP E6, Health Canada and TAHSN.

### Neuropsychological assessment

To evaluate the overall cognitive performance of participants, the Mini-Mental State Examination (MMSE) and Montreal Cognitive Assessment (MoCA) were performed. Since impairment in episodic memory is most commonly seen in MCI patients that progress to AD, a variety of episodic memory tests that assess both immediate and delayed memory recall were performed, including the Logical Memory II subscale from the Wechsler Memory Scale-Revised and the Repeatable Battery for the Assessment of Neuropsychological Status (RBANS). Given that other cognitive domains may be affected in aMCI, additional tests were performed to assess language, attention, executive function and visuospatial performance including RBANS, verbal fluency, letter number span (LNS), Stroop test and trail-making test.

### PET image acquisition

Each participant underwent a 125-min [ $^{18}\text{F}$ ]-FEPPA and a 90-min [ $^{11}\text{C}$ ]-PIB PET scan using a 3DHRRT scanner (CS/Siemens, Knoxville, TN, USA), which measures radioactivity in 207 slices with an inter-slice distance of 1.22 mm. The detectors of the HRRT are an LSO/LYSO phoswich detector, with each crystal element measuring  $2 \times 2 \times 10 \text{ mm}^3$ . Before the acquisition of the emission scan began, a transmission scan with a single photon point source,  $^{137}\text{C}$  ( $t_{1/2} = 30.2$  years,  $E\gamma = 662 \text{ keV}$ ), was acquired. The [ $^{18}\text{F}$ ]-FEPPA was 125 min in length following the injection of the radiotracer. The images were reconstructed into a series of 34 time frames including 1 frame of variable length, followed by frames comprising  $5 \times 30 \text{ s}$ ,  $1 \times 45 \text{ s}$ ,  $2 \times 60 \text{ s}$ ,  $1 \times 90 \text{ s}$ ,  $1 \times 120 \text{ s}$  and  $22 \times 300 \text{ s}$ .

Prior to the start of the PET scans, a custom fitted thermoplastic mask was made for each participant to minimize head movement. The radiosyntheses of [ $^{18}\text{F}$ ]-

FEPPA<sup>16</sup> and [ $^{11}\text{C}$ ]-PIB<sup>18</sup> have been described in detail elsewhere. For [ $^{18}\text{F}$ ]-FEPPA, an intravenous saline solution of  $4.91 \pm 0.42$  (mean  $\pm$  SD) mCi was administered as a bolus. An automated blood sampling system (ABSS, Model #PBS-101 from Veenstra Instruments, Netherlands) was used to measure arterial blood radioactivity continuously at a rate of 2.5 ml/minute for the first 22.5 minutes of the PET scan. Additionally, manual arterial samples were obtained at 2.5, 7, 12, 15, 30, 45, 60, 90 and 120 min after injection of the radiotracer. The arterial samples were used to generate an input function of unmetabolized radioligand in the plasma for kinetic analysis, as previously described.<sup>19</sup> For [ $^{11}\text{C}$ ]-PIB, an intravenous saline solution of  $9.64 \pm 0.89$  mCi was administered as a bolus. Images were reconstructed into a series of 34 frames comprising  $4 \times 15 \text{ s}$ ,  $8 \times 30 \text{ s}$ ,  $9 \times 60 \text{ s}$ ,  $2 \times 180 \text{ s}$ ,  $8 \times 300 \text{ s}$  and  $3 \times 600 \text{ s}$ .

The PD-weighted MRI scans were acquired on a 3-Tesla General Electric MR750 scanner. The MRI scans were used for co-registration of PET images, ROI delineation and partial volume correction.

### ROI-based PET image analysis

The ROIs were automatically delineated as previously described.<sup>20</sup> Grey matter ROIs known to be affected in AD were examined, including the prefrontal, temporal, inferior parietal, and occipital cortices, and the hippocampus.

To obtain a quantitative measure of [ $^{18}\text{F}$ ]-FEPPA uptake, the data were analyzed using the 2-tissue compartment model (2TCM) with total distribution volume ( $V_T$ ) as the outcome measure, as previously validated.<sup>19</sup>  $V_T$  is a ratio at equilibrium of the radioligands concentration in tissue to that in plasma (i.e. specific binding and non-displaceable uptake, which includes non-specifically bound and free radioligand in tissue). In addition to  $V_T$ , [ $^{18}\text{F}$ ]-FEPPA uptake was quantified using a supplementary method that does not involve the arterial input function, the standardized uptake value ratio (SUVR), which was correlated with the absolute quantification method in a previous sample of AD and MCI participants.<sup>21</sup> The SUVR method is based on the use of the cerebellum as a pseudo-reference region. SUVs for each region of interest were calculated by using the time activity curve (TAC) values. For each ROI, the TAC values were averaged between 90 and 120 min and multiplied by the subject's body weight and divided by the injected dose. The SUVR was then calculated by dividing the SUV of a ROI by the cerebellar SUV.

[ $^{11}\text{C}$ ]-PIB retention was measured using the Logan plot with the cerebellum as a reference region to yield distribution volume ratio (DVR), as this method has been shown to provide stable and robust results in

several ROIs.<sup>22</sup> Additionally, participants were classified by either the presence of A $\beta$  plaques (PIB-positive) or absence of A $\beta$  plaques (PIB-negative). The average DVR of the prefrontal, temporal, inferior parietal and occipital cortices was calculated, and a cut-off of 1.20 was applied to stratify participants according to PIB status.<sup>23</sup> The kinetic analysis of the radioligands was performed using an in house software (fMOD) developed by one of the co-authors (PR). To correct for age associated changes in brain volume, the activity data for all participants was corrected for the effect of partial volume error (PVE) using the Mueller–Gartner algorithm, as previously implemented.<sup>24</sup> The results of this study are reported using dynamic PET images with and without PVEC.

### DNA extraction and polymorphism genotyping

Genomic DNA was obtained from peripheral leukocytes by using high salt-extraction methods.<sup>25</sup> The TSPO polymorphism rs6971 was genotyped as previously described.<sup>26</sup> Based on their genotype, participants were classified as high-, mixed-, and low-affinity binders (HAB, MAB and LAB, respectively), as described elsewhere.<sup>26</sup> Only HABs were invited to proceed with the study.

### Statistical analysis

Statistical analyses were performed using SPSS Statistics (version 24.0, IBM, Armonk, NY, USA). Demographic variables and [<sup>18</sup>F]-FEPPA and [<sup>11</sup>C]-PIB injected parameters were compared between aMCI and healthy volunteers using an independent sample *t*-test. Regional differences in [<sup>18</sup>F]-FEPPA and [<sup>11</sup>C]-PIB bindings between the two groups were compared using a univariate analysis of variance with age added as a covariate. Spatial relationships between [<sup>18</sup>F]-FEPPA and [<sup>11</sup>C]-PIB were explored with non-parametric correlations. Non-parametric correlations were also performed to assess associations between microglial activation or A $\beta$  burden and cognition. Assessments were grouped by cognitive domain that was evaluated (memory, executive function, language, attention and overall global cognition), and subsequently Bonferroni correction was applied.

### Results

Eleven aMCI participants (age range: 60–79 years) and 14 healthy volunteers (age range: 56–78 years) completed all study procedures. Descriptive characteristics and PET parameters are presented in Table 1. There were no differences in age, gender and education amongst the two groups. As expected, aMCI

participants had significantly lower MMSE and MoCA scores than healthy volunteers. In comparison to healthy volunteers, aMCI participants had more cardiovascular risk factors such as hypertension and hypercholesterolemia. Additionally, more aMCI participants were taking antidepressants; however, none met criteria for a current diagnosis of major depressive disorder. There were no differences in the PET parameters of [<sup>18</sup>F]-FEPPA and [<sup>11</sup>C]-PIB between the two groups.

### Differences in [<sup>11</sup>C]-PIB binding between aMCI and healthy volunteers

Participants with aMCI had significantly more A $\beta$  plaque deposition than healthy volunteers in all cortical ROI (Figure 1). The largest difference in [<sup>11</sup>C]-PIB retention was observed in the prefrontal cortex, 48.6%. The order of increased A $\beta$  burden was as follows: prefrontal cortex > temporal cortex > inferior parietal cortex > occipital cortex > hippocampus. No significant differences between groups were observed in the hippocampus. Similar results were observed without correction for partial volume effects (Supplemental Figure 3). After using a cut-off for [<sup>11</sup>C]-PIB retention, 8/11 (73%) of aMCI patients were characterized as PIB-positive, whereas only 3/14 (21%) of healthy volunteers had significant A $\beta$  plaque accumulation. Parametric images of [<sup>11</sup>C]-PIB SUVR (40–90 min) were created to visually represent the differences between the healthy volunteers and aMCI participants (Supplemental Figure 2).

### Differences in [<sup>18</sup>F]-FEPPA $V_T$ between aMCI and healthy volunteers

No significant differences in [<sup>18</sup>F]-FEPPA binding were observed between aMCI participants and healthy volunteers in any of the ROI (Figure 2). Large overlaps in  $V_T$  were observed between the two groups in each region of interest. Percent differences between the groups (healthy volunteers vs. aMCI) were estimated at 0.27%, –1.40%, –0.09%, 0.64% and 16.17% in the temporal, prefrontal, inferior parietal, occipital and hippocampus, respectively. Similarly, the supplementary SUVR method did not yield any significant group differences (Supplemental Table 1). Although not significant, the overall percent differences between the two groups are larger with the SUVR method, ranging from 4.01% in the inferior parietal cortex to 12.04% in the hippocampus, with partial volume correction. To visually represent the data, parametric images of [<sup>18</sup>F]-FEPPA  $V_T$  were created (Supplemental Figure 1).

Between the two aMCI groups (i.e. PIB-negative and PIB-positive), participants with amyloid pathology had

**Table 1.** Participants' demographics and PET parameters (mean  $\pm$  SD).

	HV ( <i>n</i> = 14)	aMCI ( <i>n</i> = 11)	
Age (years)	67.07 $\pm$ 6.49	71.91 $\pm$ 5.30	<i>t</i> = 1.59, <i>p</i> = 0.13
Gender			
Female	9	6	$\chi^2$ = 0.24, <i>p</i> = 0.62
Male	5	5	
Education (years)	16.21 $\pm$ 3.40	15.82 $\pm$ 2.36	<i>t</i> = -0.33, <i>p</i> = 0.75
MMSE	29.3 $\pm$ 1.25	27.3 $\pm$ 1.95*	<i>t</i> = -2.80, <i>p</i> = 0.01
MoCA	27.0 $\pm$ 1.4	21.7 $\pm$ 3.6*	<i>t</i> = -4.63, <i>p</i> = 0.001
Concurrent			
Cholinesterase inhibitors	0	2	
Medications			
Antihypertensives	1	5	
Statins	1	3	
Antidepressants	0	6	
Baby aspirin	1	1	
[ <sup>18</sup> F]-FEPPA			
Amount injected (mCi)	4.99 $\pm$ 0.25	4.81 $\pm$ 0.56	<i>t</i> = -1.04, <i>p</i> = 0.31
Specific activity (mCi/ $\mu$ mol)	2868.56 $\pm$ 2120.49	1960.49 $\pm$ 1481.40	<i>t</i> = -1.21, <i>p</i> = 0.24
Mass injected ( $\mu$ g)	1.22 $\pm$ 1.16	1.42 $\pm$ 0.83	<i>t</i> = 0.48, <i>p</i> = 0.64
[ <sup>11</sup> C]-PIB			
Amount injected (mCi)	9.47 $\pm$ 1.04	9.87 $\pm$ 0.66	<i>t</i> = 1.18, <i>p</i> = 0.25
Specific activity (mCi/ $\mu$ mol)	1892.86 $\pm$ 1029.12	2135.01 $\pm$ 1122.85	<i>t</i> = 0.56, <i>p</i> = 0.58
Mass injected ( $\mu$ g)	1.90 $\pm$ 1.07	1.43 $\pm$ 0.59	<i>t</i> = -1.30, <i>p</i> = 0.21

aMCI: amnesic mild cognitive impairment; HV: healthy volunteer; MMSE: mini-mental state examination; MoCA: Montreal cognitive assessment; SD: standard deviation.

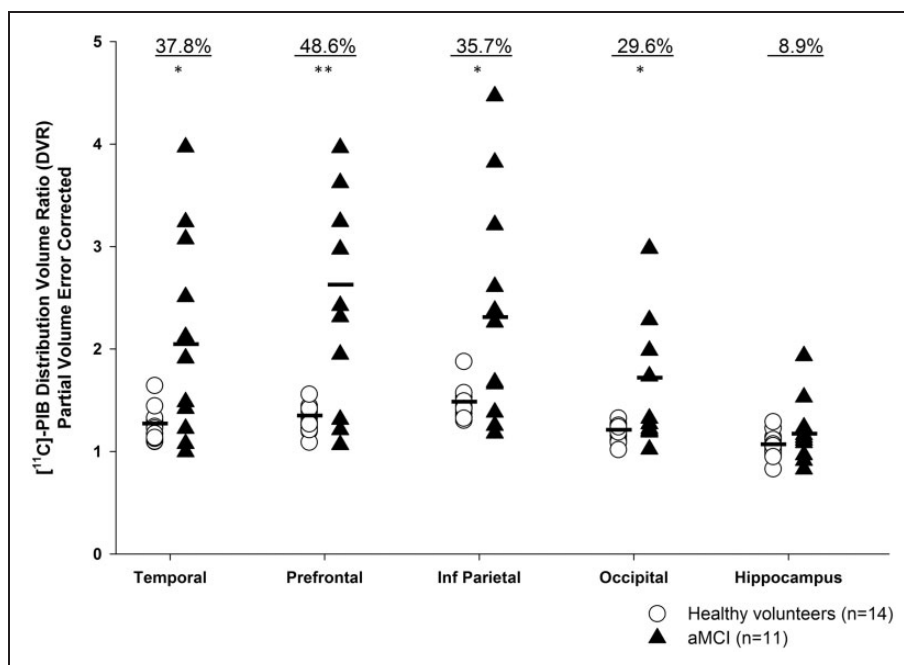


**Figure 1.** [<sup>11</sup>C]-PIB distribution value ratios (DVR) in regions of interest with partial volume correction. aMCI participants (*n* = 11) had higher [<sup>11</sup>C]-PIB binding in all regions except hippocampus. \**p*  $\leq$  0.05, \*\**p* < 0.01. The percent differences in binding are shown above each ROI.

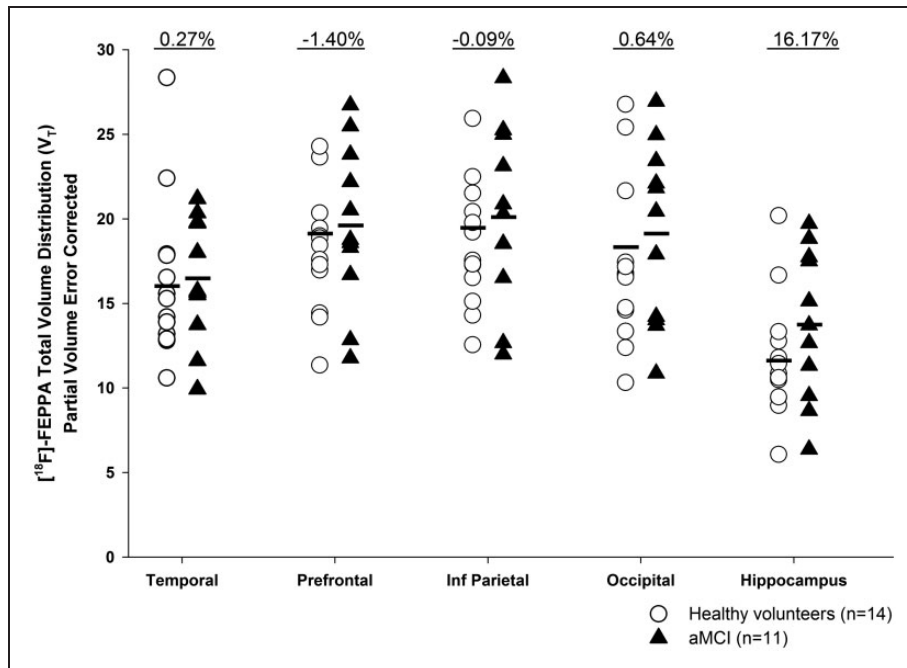


**Figure 2.** [ $^{18}\text{F}$ ]-FEPPA total volume distribution ( $V_T$ ) in regions of interest with partial volume correction. No significant differences were observed between aMCI participants ( $n = 11$ ) and healthy volunteers ( $n = 14$ ). The percent differences in binding are shown above each ROI.

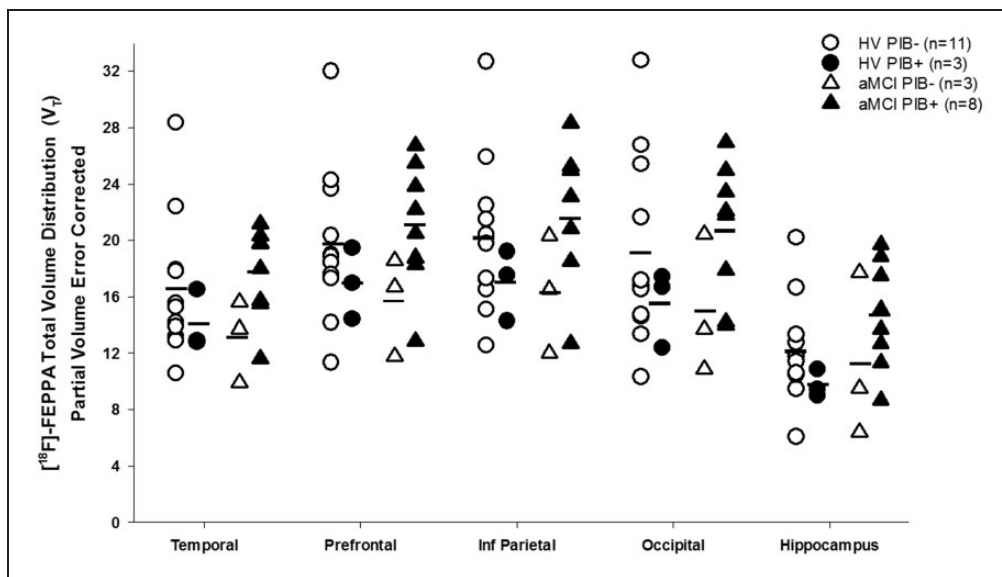


**Figure 3.** Regional [ $^{18}\text{F}$ ]-FEPPA  $V_T$  for healthy volunteers and aMCI participants when stratified by PIB status. An average of 1.20 DVR in the cortical regions was used as a cut-off.<sup>23</sup> No significant differences were observed between groups. PIB+=PIB-positive; PIB-=PIB-negative.

higher [ $^{18}\text{F}$ ]-FEPPA binding in all ROI; however, the difference was not significant (Figure 3, Supplemental Table 2). As commonly done in PET studies, when PIB-negative healthy volunteers were compared to PIB-positive aMCI participants, the percent differences

observed were 5.97% in the temporal cortex, 4.14% in the prefrontal cortex, 5.43% in the inferior parietal cortex, 5.9% in the occipital cortex and 23.21% in the hippocampus. The differences are not significant and similar to those obtained with the SUVR method.

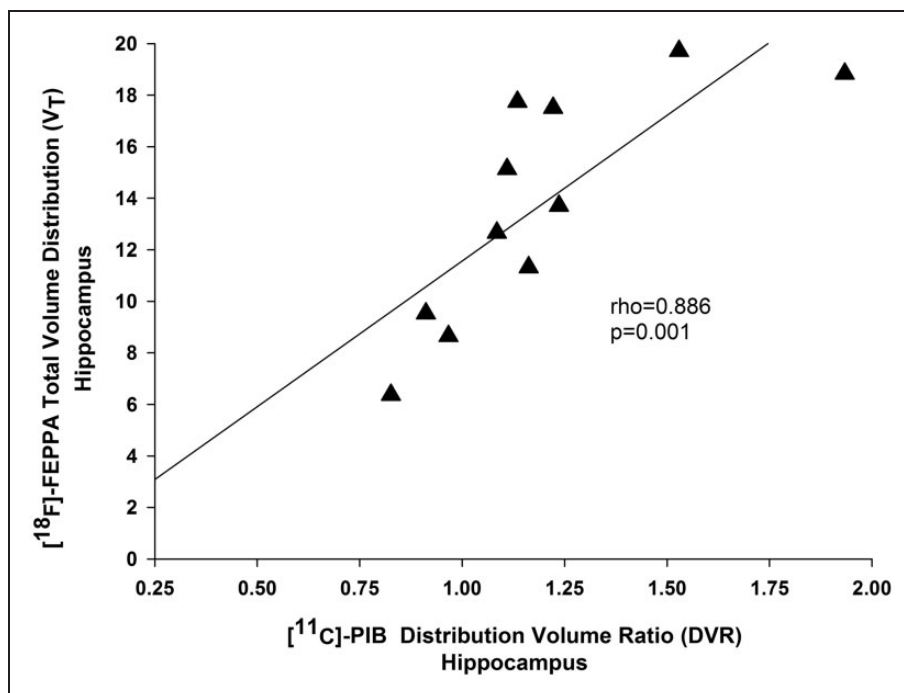


**Figure 4.** Regional association between [<sup>18</sup>F]-FEPPA and [<sup>11</sup>C]-PIB binding in the hippocampus. The correlation is shown in aMCI participants ( $n = 11$ ) and after partial volume correction. The correlation in the hippocampus survived after Bonferroni correction for multiple comparisons.

#### Exploratory correlations between [<sup>18</sup>F]-FEPPA $V_T$ , [<sup>11</sup>C]-PIB binding and cognition

In aMCI participants, a Bonferroni corrected spatial correlation between [<sup>11</sup>C]-PIB binding and [<sup>18</sup>F]-FEPPA binding was observed in the hippocampus ( $\rho = 0.886$ ,  $p = 0.001$ ) (Figure 4). A similar correlation was observed before partial volume correction (Supplemental Figure 5). In terms of cognition, we did not find any correlation between cognitive measures and either [<sup>11</sup>C]-PIB retention or [<sup>18</sup>F]-FEPPA binding in our aMCI group (Supplemental Tables 4 and 5).

## Discussion

From our dual-tracer PET study, we found that amyloid, but not neuroinflammation, is evident in prodromal AD individuals. aMCI participants had significantly more A $\beta$  plaques, as indexed by [<sup>11</sup>C]-PIB, in the cortical regions. Our observed distribution pattern of [<sup>11</sup>C]-PIB retention is consistent with the pattern of A $\beta$  plaque deposition observed in post-mortem studies of the AD brain,<sup>27,28</sup> whereby studies have shown large increases in neuritic plaques in cortical regions and lower levels in the medial temporal cortex, including the hippocampus. Furthermore, PET studies of MCI and AD patients have similarly reported increases in [<sup>11</sup>C]-PIB retention in the cortical regions and lower

levels in the hippocampus.<sup>4,6,15,29–31</sup> The idea that aMCI patients fall into the intermediate range of PIB retention is supported by reports of patients being characterized as PIB-positive or PIB-negative. The presence of A $\beta$  in the majority of our aMCI patients (73%) is supported by other PET studies that have demonstrated an increase in A $\beta$  in 50–75% of aMCI patients.<sup>4,6,31</sup> Conversely, only 3/14 (or 21%) of our healthy volunteers were characterized as PIB-positive, with the majority being classified as PIB-negative. Increased amyloid deposition has been reported in up to one-third of cognitively normal elderly participants,<sup>32</sup> which explains the finding of increased [<sup>11</sup>C]-PIB binding in three of our healthy volunteers.

In contrast to amyloid pathology, we did not observe a significant difference in [<sup>18</sup>F]-FEPPA binding between aMCI and healthy volunteers in any region of interest with either the absolute quantification method, 2TCM, or the supplementary SUVR method, suggesting that neuroinflammatory processes may become predominant later during disease progression. Although not significant, the 16.7% difference in [<sup>18</sup>F]-FEPPA binding in the hippocampus may be of clinical significance. A previous study with [<sup>18</sup>F]-FEPPA in AD patients similarly observed the largest difference in binding in the hippocampus of AD patients. In the HAB only group, the percent difference between the AD group and healthy volunteers was 63%.<sup>1</sup>

Similarly to our study, Kreisl et al.<sup>9</sup> did not find a statistical difference in [<sup>11</sup>C]-PBR28 binding between MCI and healthy volunteers. Interestingly, the largest difference in [<sup>11</sup>C]-PBR28 binding between these two groups was also in the hippocampus (non-significant). We can speculate that the hippocampus may be one of the regions with the earliest microglial changes. As the disease progresses, microglia may then spread and increase in other regions as observed in the increased [<sup>18</sup>F]-FEPPA in various grey and white matter regions of AD patients.<sup>1</sup> The significance of the hippocampus is also evident in our finding of a positive correlation between [<sup>18</sup>F]-FEPPA and [<sup>11</sup>C]-PIB in the aMCI group. While this region did not have an increase in [<sup>11</sup>C]-PIB binding in aMCI compared to healthy volunteer, this result suggests that the amyloid plaques are spatially correlated with microglial cells. We can further speculate that another key pathological feature of AD, tau neurofibrillary tangles, may be playing a role in our findings for several reasons. Post-mortem AD samples have shown that the spread and deposition of tau begin in the hippocampus prior to the cortical regions.<sup>33</sup> Similarly to amyloid, tau has been shown to activate microglial cells. The relationship between the two is further supported by evidence of the role of microglia in tau propagation.<sup>34</sup> Taken together, we can hypothesize that the early increase in [<sup>18</sup>F]-FEPPA in the hippocampus may be a result of the early tau accumulation evidenced in aMCI patients. Our hypothesis is limited by the fact that hippocampus is a small region that is more susceptible to noise. However, given that the correlation was observed before and after correction for partial volume effects, we can be more assured of the possible clinical significance of this region.

Previous PET studies investigating neuroinflammation in MCI participants have observed conflicting results, with some reporting no differences from healthy volunteers,<sup>4,5,9</sup> while others reported increased neuroinflammation in certain regions.<sup>6,8</sup> These inconsistent results observed in PET studies investigating neuroinflammation in MCI participants are partially due to notable differences in methodology and demographic characteristics between studies. Three of the studies have used the prototypical radioligand, [<sup>11</sup>C]-PK11195, which has several limitations including a short half-life, low specific to non-specific binding, low brain penetration and high plasma protein binding.<sup>4-6</sup> Furthermore, two of the studies did not use a purely amnesic sample of MCI patients,<sup>4,8</sup> which increases heterogeneity as MCI is a broad category that may encompass a multitude of underlying pathologies. The previous two studies with second-generation radioligands report conflicting results. A study with [<sup>11</sup>C]-DAA1106 in a sample of 5 aMCI and 2 non-amnesic MCI participants reported increased binding

in certain ROIs,<sup>8</sup> whereas a study with [<sup>11</sup>C]-PBR28 in 10 aMCI participants (4 HAB and 6 MAB) did not observe any significant differences in binding from healthy volunteers.<sup>9</sup> However, the sample size for the HAB group was very small. Our results are congruent with and expand on the latter study that similarly included only aMCI participants. Taking our results together with previous PET studies that have demonstrated an increase in TSPO binding in AD patients and two recent longitudinal studies that demonstrated an increase in TSPO binding during clinical progression,<sup>10,35</sup> we can speculate that neuroinflammation only becomes evident during later stages of disease progress.

In terms of the relationship between amyloid and neuroinflammation, a previous study examining aMCI patients specifically observed an elevation in [<sup>11</sup>C]-PK11195 binding in patients with increased PIB retention.<sup>6</sup> Similarly, in our aMCI sample, those that were PIB-positive had higher [<sup>18</sup>F]-FEPPA binding in the prefrontal, temporal, inferior parietal and occipital cortices compared to aMCI patients classified as PIB-negative (albeit not significantly). Our finding of a regional association between [<sup>11</sup>C]-PIB and [<sup>18</sup>F]-FEPPA in the hippocampus is in contrast to some PET studies that have demonstrated no significant correlations between [<sup>11</sup>C]-PK11195 and [<sup>11</sup>C]-PIB in AD and/or MCI patients.<sup>4,6,15</sup> The negative results observed by these previous studies may in part be due to the use of [<sup>11</sup>C]-PK11195 and simplified reference tissue models rather than a full kinetic model with an arterial input function. So far only one other study has evaluated the spatial relationship of amyloid and neuroinflammation in MCI with the use of a second-generation radioligand and the full kinetic model with an arterial input function. This study reported a significant correlation between [<sup>11</sup>C]-PBR28 and [<sup>11</sup>C]-PIB in the inferior parietal lobule, superior temporal cortex, precuneus, hippocampus and parahippocampal gyrus.<sup>9</sup> Nonetheless, these correlations were observed only after correction for partial volume effects and when AD and MCI populations were combined. Our study is the first to report a spatial relationship between A $\beta$  deposition and neuroinflammation in the largest sample of HAB aMCI.

Finally, in our exploratory analyses, [<sup>11</sup>C]-PIB binding was not correlated with any of the cognitive assessments. Our result is in line with post-mortem studies of AD that have generally demonstrated that amyloid does not correlate well with symptom severity or cognitive impairment.<sup>36-38</sup> Whereas in-vivo PET studies have reported conflicting results, with some groups demonstrating no correlations between [<sup>11</sup>C]-PIB retention and performance on cognitive scales,<sup>6,39,40</sup> while others report correlations with an impairment in



episodic memory.<sup>41–43</sup> Previous studies have shown divergent results regarding the relationship between neuroinflammation and cognition.<sup>1,5,6,8,9,15</sup> In MCI studies specifically, only one study has reported a significant correlation between cognitive function and neuroinflammation, suggesting that higher neuroinflammation in the inferior parietal lobule was associated with higher scores on CDR and Block design.<sup>9</sup> However, the authors combined the AD and MCI participants into one group, meaning that the correlations may be driven by the AD subgroup. Other MCI studies report no correlations with cognition.<sup>5,6,8</sup> Similarly, we did not observe any correlations between [<sup>18</sup>F]-FEPPA and cognition. Overall, it is likely that impairments in cognition are influenced by additional pathology such as the presence or absence of neurofibrillary tangles, thus explaining the inconsistencies in results.<sup>6</sup>

As with most studies, certain limitations need to be considered. Firstly, our sample size was relatively small; however, the inclusion of only HABs reduces the variability of the sample hence reporting the largest homogeneous aMCI cohort in the literature. The inclusion of only HABs is further supported by a previous study that investigated whether the TSPO genotype influences cognitive function, amyloid load, and disease progression over time. The researchers demonstrated that there were no differences between the three TSPO groups and concluded that the information obtained from evaluating a subgroup of AD or MCI subjects can be translated to the entire AD and MCI population.<sup>44</sup> However, while the inclusion of one TSPO genetic group reduces the variability in [<sup>18</sup>F]-FEPPA binding, a significant drawback to this preselection is the difficulty that arises with recruitment. Conducting a PET study with elderly, frail individuals already has some inherent difficulties given that many are hesitant to undergo a 2 h scan with arterial blood sampling. Over half of the consented MCI participants in our study had to be discharged early following the genetic screening. This demonstrates that while there are advantages to studying a genetically homogeneous sample, large resources for recruitment will need to be utilized in order to have a sufficient sample size.

Another limitation is that although an increase in [<sup>18</sup>F]-FEPPA binding is mostly attributed to microglial activation, studies show that astrocytes also express TSPO.<sup>9</sup> Thus, [<sup>18</sup>F]-FEPPA binding may also be indicating the presence of reactive astrocytes in the brain. Another consideration is that TSPO radioligands do not differentiate between the two phenotypes of microglia, M1 and M2, which are pro-inflammatory and anti-inflammatory (neuroprotective), respectively.<sup>10</sup>

Although the aMCI participants did not meet criteria for current Axis I disorder, 6 of the 11 participants

were taking antidepressants. There is some evidence that antidepressants can alter the inflammatory potential of microglia; however, there is no evidence that they can affect TSPO radioligand binding. Our recent study investigating [<sup>18</sup>F]-FEPPA binding in AD, that similarly included patients taking SSRIs, reported that differences in [<sup>18</sup>F]-FEPPA binding remained significant in all gray matter and white matter ROI even after excluding those on antidepressants.<sup>1</sup> Similarly, within our sample, no differences in [<sup>18</sup>F]-FEPPA binding were observed between aMCI participants on antidepressants ( $n=6$ ) when compared to those not taking anti-depressant medications ( $n=5$ ).

Finally, we did not calculate the plasma free fraction ( $f_p$ ) values for [<sup>18</sup>F]-FEPPA. It is important to note that the calculation of  $f_p$  is difficult for TSPO radioligands and values can themselves vary due to methodological differences and measurement inaccuracies.<sup>45,46</sup> This is in part due to the fact that  $f_p$  of certain PET tracers is very low (<5%).<sup>45</sup> A previous study with [<sup>18</sup>F]-FEPPA in AD did not correct for  $f_p$  and yet the researchers were still able to detect significant increases in AD patients compared to healthy volunteers, thus we can be more assured in our results. In order to overcome the difficulties with the absolute quantification method, groups have estimated TSPO binding with alternative methods, one of which is the use of the cerebellum as a pseudo-reference region. A previous study with [<sup>11</sup>C]-PBR28 in AD and MCI participants demonstrated that the SUVR method detected greater binding in AD patients, but not in MCI, compared to healthy volunteers.<sup>21</sup> Similarly in our MCI sample, we did not observe an increase in [<sup>18</sup>F]-FEPPA binding with the SUVR method.

## Conclusion

In conclusion, this is the first study to investigate microglial activation and A $\beta$  burden in aMCI and healthy volunteers using an HRRT scanner and in only high-affinity binders. Our findings indicate that A $\beta$  deposition is an early pathological event, while neuroinflammation may occur later during the progression to AD. We further suggest that early microglial changes may become evident in the hippocampus and then spread to other regions during disease progression; however, larger studies and dual-tracer neuroinflammation-tau PET studies will be required to investigate this hypothesis.

## Funding

The author(s) disclosed receipt of the following financial support for the research, authorship, and/or publication of this article: This work was supported by The W. Garfield Weston Foundation.

## Acknowledgments

The authors would like to thank Alvina Ng, Laura Nguyen and Anusha Ravichandran for help with scanning. We would also like to thank the Baycrest and CAMH Memory Clinics, and all the participants and their families.

## Declaration of conflicting interests

The author(s) declared no potential conflicts of interest with respect to the research, authorship, and/or publication of this article.

## Authors' contributions

Dunja Knezevic: acquisition of data, analysis and interpretation of data, drafted the manuscript.

Nicolaas Paul LG Verhoeff: acquisition of data, critical revision of manuscript for intellectual content.

Sina Hafizi: analysis and interpretation of data, critical revision of manuscript for intellectual content.

Antonio Strafella: acquisition of data, critical revision for intellectual content.

Ariel Graff-Guerrero: acquisition of data, critical revision of manuscript for intellectual content.

Tarek Rajji: acquisition of data, critical revision for intellectual content.

Bruce Pollock: study concept and design, critical revision for intellectual content.

Sylvain Houle: study concept and design, critical revision for intellectual content.

Pablo Rusjan: analysis and interpretation of data, methodological PET supervision of data analyses, critical revision for intellectual content.

Romina Mizrahi: study concept and design, critical revision for intellectual content, acquisition of funding, overall study supervision.

## Supplementary material

Supplementary material for this paper can be found at the journal website: <http://journals.sagepub.com/home/jcb>

## References

- Suridjan I, Pollock B, Verhoeff N, et al. In-vivo imaging of grey and white matter neuroinflammation in Alzheimer's disease: a positron emission tomography study with a novel radioligand, [<sup>18</sup>F]-FEPPA. *Mol Psychia* 2015; 20: 1–9.
- Petersen RC, Parisi JE, Dickson DW, et al. Neuropathologic features of amnesic mild cognitive impairment. *Arch Neurol* 2006; 63: 665–672.
- Gauthier S, Reisberg B, Zaudig M, et al. Mild cognitive impairment. *Lancet* 2006; 367: 1262–1270.
- Wiley CA, Lopresti BJ, Venetti S, et al. Carbon 11-labeled Pittsburgh compound b and carbon 11-labeled (R)-PK11195 positron emission tomographic imaging in Alzheimer Disease. *Arch Neurol* 2009; 66: 60–67.
- Schuitmaker A, Kropholler MA, Boellaard R, et al. Microglial activation in Alzheimer's disease: an (R)-[11C] PK11195 positron emission tomography study. *Neurobiol Aging* 2013; 34: 128–136.
- Okello A, Edison P, Archer H, et al. Microglial activation and amyloid deposition in mild cognitive impairment A PET study. *Neurology* 2009; 72: 56–62.
- Owen DR, Yeo AJ, Gunn RN, et al. An 18-kDa translocator protein (TSPO) polymorphism explains differences in binding affinity of the PET radioligand PBR28. *J Cereb Blood Flow Metab* 2012; 32: 1–5.
- Yasuno F, Kosaka J, Ota M, et al. Increased binding of peripheral benzodiazepine receptor in mild cognitive impairment–dementia converters measured by positron emission tomography with [11 C] DAA1106. *Psychiat Res* 2012; 203: 67–74.
- Kreisl WC, Lyoo CH, McGwier M, et al. In vivo radioligand binding to translocator protein correlates with severity of Alzheimer's disease. *Brain* 2013; 136: 2228–2238.
- Hamelin L, Lagarde J, Dorothee G, et al. Early and protective microglial activation in Alzheimer's disease: a prospective study using <sup>18</sup>F-DPA-714 PET imaging. *Brain* 2016; 139: 1252–1264.
- McGeer EG and McGeer PL. Neuroinflammation in Alzheimer's disease and mild cognitive impairment: a field in its infancy. *J Alzheimers Dis* 2010; 19: 355–361.
- Rogers J, Luber-Narod J, Styren SD and Civin WH. Expression of immune system-associated antigens by cells of the human central nervous system: relationship to the pathology of Alzheimer's disease. *Neurobiol Aging* 1988; 9: 339–349.
- Itagaki S, McGeer P, Akiyama H, et al. Relationship of microglia and astrocytes to amyloid deposits of Alzheimer disease. *J Neuroimmunol* 1989; 24: 173–182.
- McGeer P, Akiyama H, Itagaki S, et al. Activation of the classical complement pathway in brain tissue of Alzheimer patients. *Neurosci Lett* 1989; 107: 341–346.
- Edison P, Archer HA, Gerhard A, et al. Microglia, amyloid, and cognition in Alzheimer's disease: an [11C](R) PK11195-PET and [11C] PIB-PET study. *Neurobiol Dis* 2008; 32: 412–419.
- Wilson AA, Garcia A, Parkes J, et al. Radiosynthesis and initial evaluation of [18 F]-FEPPA for PET imaging of peripheral benzodiazepine receptors. *Nucl Med Biol* 2008; 35: 305–314.
- Petersen RC. Mild cognitive impairment as a diagnostic entity. *J Intern Med* 2004; 256: 183–194.
- Mathis CA, Bacskai BJ, Kajdasz ST, et al. A lipophilic thioflavin-T derivative for positron emission tomography (PET) imaging of amyloid in brain. *Bioorg Med Chem Lett* 2002; 12: 295–298.
- Rusjan PM, Wilson AA, Bloomfield PM, et al. Quantitation of translocator protein binding in human brain with the novel radioligand [18F]-FEPPA and positron emission tomography. *J Cereb Blood F Met* 2011; 31: 1807–1816.
- Rusjan P, Mamo D, Ginovart N, et al. An automated method for the extraction of regional data from PET images. *Psychiatry research* 2006; 147: 79–89.
- Lyoo CH, Ikawa M, Liow JS, et al. Cerebellum Can Serve As a Pseudo-Reference Region in Alzheimer Disease to Detect Neuroinflammation Measured with

- PET Radioligand Binding to Translocator Protein. *J Nucl Med* 2015; 56: 701–706.
22. Lopresti BJ, Klunk WE, Mathis CA, et al. Simplified quantification of Pittsburgh Compound B amyloid imaging PET studies: a comparative analysis. *J Nucl Med* 2005; 46: 1959–1972.
  23. Villeneuve S, Rabinovici GD, Cohn-Sheehy BI, et al. Existing Pittsburgh Compound-B positron emission tomography thresholds are too high: statistical and pathological evaluation. *Brain* 2015; 138: 2020–2033.
  24. Müller-Gärtner HW, Links JM, Prince JL, et al. Measurement of radiotracer concentration in brain gray matter using positron emission tomography: MRI-based correction for partial volume effects. *J Cereb Blood F Met* 12: 571–583.
  25. Lahiri DK and Nurnberger JI, Jr. A rapid non-enzymatic method for the preparation of HMW DNA from blood for RFLP studies. *Nucleic Acids Res* 1991; 19: 5444.
  26. Mizrahi R, Rusjan PM, Kennedy J, et al. Translocator protein (18 kDa) polymorphism (rs6971) explains in-vivo brain binding affinity of the PET radioligand [18F]-FEPPA. *J Cereb Blood F Met* 2012; 32: 968–972.
  27. Arnold SE, Hyman BT, Flory J, et al. The topographical and neuroanatomical distribution of neurofibrillary tangles and neuritic plaques in the cerebral cortex of patients with Alzheimer's disease. *Cereb Cortex* 1991; 1: 103–116.
  28. Thal DR, Rüb U, Orantes M, et al. Phases of A $\beta$ -deposition in the human brain and its relevance for the development of AD. *Neurology* 2002; 58: 1791–1800.
  29. Klunk WE, Engler H, Nordberg A, et al. Imaging brain amyloid in Alzheimer's disease with Pittsburgh Compound-B. *Ann Neurol* 2004; 55: 306–319.
  30. Lopresti BJ, Klunk WE, Mathis CA, et al. Simplified quantification of Pittsburgh Compound B amyloid imaging PET studies: a comparative analysis. *J Nucl Med* 2005; 46: 1959–1972.
  31. Rowe CC, Ng S, Ackermann U, et al. Imaging beta-amyloid burden in aging and dementia. *Neurology* 2007; 68: 1718–1725.
  32. Mintun MA, Larossa GN, Sheline YI, et al. [11C]PIB in a nondemented population: potential antecedent marker of Alzheimer disease. *Neurology* 2006; 67: 446–452.
  33. Braak H and Braak E. Frequency of stages of Alzheimer-related lesions in different age categories. *Neurobiol Aging* 1997; 18: 351–357.
  34. Asai H, Ikezu S, Tsunoda S, et al. Depletion of microglia and inhibition of exosome synthesis halt tau propagation. *Nature Neurosci* 2015; 18: 1584–1593.
  35. Varrone A and Nordberg A. Molecular imaging of neuroinflammation in Alzheimer's disease. *Clin Transl Imaging* 2015; 3: 437–447.
  36. Arriagada PV, Growdon JH, Hedley-Whyte ET, et al. Neurofibrillary tangles but not senile plaques parallel duration and severity of Alzheimer's disease. *Neurology* 1992; 42: 631–631.
  37. Bierer LM, Hof PR, Purohit DP, et al. Neocortical neurofibrillary tangles correlate with dementia severity in Alzheimer's disease. *Arch Neurol* 1995; 52: 81–88.
  38. Vehmas AK, Kawas CH, Stewart WF, et al. Immune reactive cells in senile plaques and cognitive decline in Alzheimer's disease. *Neurobiol Aging* 2003; 24: 321–331.
  39. Edison P, Archer HA, Hinz R, et al. Amyloid, hypometabolism, and cognition in Alzheimer disease: an [11C]PIB and [18F]FDG PET study. *Neurology* 2007; 68: 501–508.
  40. Jack CR, Jr., Lowe VJ, Senjem ML, et al. 11C PiB and structural MRI provide complementary information in imaging of Alzheimer's disease and amnesic mild cognitive impairment. *Brain* 2008; 131: 665–680.
  41. Pike KE, Savage G, Villemagne VL, et al. Beta-amyloid imaging and memory in non-demented individuals: evidence for preclinical Alzheimer's disease. *Brain* 2007; 130: 2837–2844.
  42. Forsberg A, Engler H, Almkvist O, et al. PET imaging of amyloid deposition in patients with mild cognitive impairment. *Neurobiol Aging* 2008; 29: 1456–1465.
  43. Villemagne VL, Pike KE, Chételat G, et al. Longitudinal assessment of A $\beta$  and cognition in aging and Alzheimer disease. *Ann Neurol* 2011; 69: 181–192.
  44. Fan Z, Harold D, Pasqualetti G, et al. Can studies of neuroinflammation in a TSPO genetic subgroup (HAB or MAB) be applied to the entire AD cohort? *J Nucl Med* 2015; 56: 707–713.
  45. Turkheimer F, Rizzo G, Bloomfield PS, et al. The methodology of TSPO imaging with positron emission tomography. *Biochem Soc Trans* 2015; 43: 586–592.
  46. Albrecht DS, Granziera C, Hooker JM, et al. In vivo imaging of human neuroinflammation. *ACS Chem Neurosci* 2016; 7: 470–483.